ARTICLE

Corrected: Publisher Correction

https://doi.org/10.1038/s41586-018-0600-6

Antibody and TLR7 agonist delay viral rebound in SHIV-infected monkeys

Erica N. Borducchi[1,6], Jinyan Liu[1,6], Joseph P. Nkolola[1,6], Anthony M. Cadena[1,6], Wen-Han Yu[2], Stephanie Fischinger[2], Thomas Broge[2], Peter Abbink[1], Noe B. Mercado[1], Abishek Chandrashekar[1], David Jetton[1], Lauren Peter[1], Katherine McMahan[1], Edward T. Moseley[1], Elena Bekerman[3], Joseph Hesselgesser[3], Wenjun Li[4], Mark G. Lewis[5], Galit Alter[2], Romas Geleziunas[3] & Dan H. Barouch[1,2]*

The latent viral reservoir is the critical barrier for the development of a cure for HIV-1 infection. Previous studies have shown direct antiviral activity of potent HIV-1 Env-specific broadly neutralizing antibodies (bNAbs) administered when antiretroviral therapy (ART) was discontinued, but it remains unclear whether bNAbs can target the viral reservoir during ART. Here we show that administration of the V3 glycan-dependent bNAb PGT121 together with the Toll-like receptor 7 (TLR7) agonist vesatolimod (GS-9620) during ART delayed viral rebound following discontinuation of ART in simian-human immunodeficiency virus (SHIV)-SF162P3-infected rhesus monkeys in which ART was initiated during early acute infection. Moreover, in the subset of monkeys that were treated with both PGT121 and GS-9620 and that did not show viral rebound after discontinuation of ART, adoptive transfer studies and CD8-depletion studies also did not reveal virus. These data demonstrate the potential of bNAb administration together with innate immune stimulation as a possible strategy for targeting the viral reservoir.

The viral reservoir in latently infected $CD4^+$ T lymphocytes[1–4] is responsible for viral rebound in the vast majority of HIV-1-infected individuals who stop taking ART and represents the key challenge to a cure for HIV-1 infection[5,6]. Multiple strategies for an HIV-1 cure are currently being pursued. One hypothesis is that activation of reservoir cells may render them more susceptible to immune-mediated destruction[7–9], but, to our knowledge, direct evidence that this strategy can reduce the viral reservoir in vivo has not previously been reported.

Potent HIV-1-specific bNAbs have been shown to reduce viraemia in untreated, chronically SHIV-infected rhesus monkeys[10–12] and in HIV-1-infected humans[13,14]. Moreover, bNAbs have been reported to delay viral rebound in HIV-1-infected humans when the antibodies were administered at the time of discontinuation of ART[15,16]. These studies demonstrate that bNAbs can exert direct antiviral activity, but whether they can target the viral reservoir during ART suppression remains to be determined. Such an experiment would require that bNAbs no longer be present at therapeutic levels when ART is discontinued. To explore this concept, we evaluated the capacity of the potent neutralizing antibody PGT121[17,18] and the TLR7 agonist vesatolimod (GS-9620)[19,20] to target the viral reservoir in ART-suppressed, SHIV-SF162P3-infected rhesus monkeys.

Study design

We infected 44 Indian-origin rhesus monkeys (*Macaca mulatta*) by the intrarectal route with our rhesus peripheral blood mononuclear cell (PBMC)-derived stock of SHIV-SF162P3[21] and initiated daily subcutaneous administration of a pre-formulated ART cocktail (tenofovir disoproxil fumarate, emtricitabine, dolutegravir)[20] on day 7 of infection (Extended Data Fig. 1). Monkeys had median plasma viral loads of 4.2–4.3 log RNA copies per ml (range 2.8–5.8 log RNA copies per ml) on day 7 before initiation of ART (Fig. 1a). Viral loads were balanced among the different groups. Following initiation of ART, plasma viraemia declined to undetectable levels in most monkeys by week 3 and in all monkeys by week 6.

All monkeys were treated with continuous daily ART for 96 weeks and then received one of the following interventions ($n = 11$ monkeys per group; Fig. 1b, Extended Data Fig. 1): sham (group 1), GS-9620 alone (group 2), PGT121 alone (group 3), or both PGT121 and GS-9620 (group 4). In groups 2 and 4, monkeys received ten oral administrations of 0.15 mg kg^{-1} GS-9620 (Gilead Sciences) every two weeks from weeks 96 to 114. In groups 3 and 4, monkeys received five intravenous infusions of 10 mg kg^{-1} PGT121 (Catalent Biopharma) every two weeks from weeks 106 to 114. Thus, in the combination group, monkeys first received five doses of GS-9620 alone and then received five doses of both PGT121 and GS-9620. ART was continued for 16 weeks after the final administration of PGT121 and GS-9620 to allow antibody washout before discontinuation of ART at week 130. Viral loads remained undetectable in all monkeys throughout the period of ART suppression with no evidence of viral 'blips' to week 130 (Fig. 1b).

Pharmacodynamics and pharmacokinetics

Triggering of TLR7 leads to innate immune activation[22,23], and we previously reported that treatment with the TLR7 agonist GS-986 resulted in robust $CD4^+$ T cell activation in rhesus monkeys[20]. In the present study, the related TLR7 agonist GS-9620 similarly led to activation of $CD4^+$ T cells, as evidenced by increased CD69 and CD38 expression on $CD4^+$ T cells on the day after each GS-9620 administration (Fig. 2a, Extended Data Fig. 2a; $P = 0.001$–0.03, Mann–Whitney tests). Moreover, GS-9620 activated natural killer (NK) cells (Fig. 2b; $P = 0.001$–0.01, Mann–Whitney tests) and monocytes (data not shown), and led to increased plasma levels of IFNα, IL-1RA, I-TAC, eotaxin, MIG, MCP-1, IL-1β, IL-6 and IP-10 (Extended Data Fig. 2b).

PGT121 was detected in serum after each of the five infusions from weeks 106 to 114 without evidence of induction of anti-drug antibodies (Extended Data Figs. 3, 4a). After the final PGT121 infusion, PGT121 levels fell rapidly, reflecting the short half-life of this human

[1]Center for Virology and Vaccine Research, Beth Israel Deaconess Medical Center, Harvard Medical School, Boston, MA, USA. [2]Ragon Institute of MGH, MIT, and Harvard, Cambridge, MA, USA. [3]Gilead Sciences, Foster City, CA, USA. [4]University of Massachusetts Medical School, Worcester, MA, USA. [5]Bioqual, Rockville, MD, USA. [6]These authors contributed equally: Erica N. Borducchi, Jinyan Liu, Joseph P. Nkolola, Anthony M. Cadena. *e-mail: dbarouch@bidmc.harvard.edu

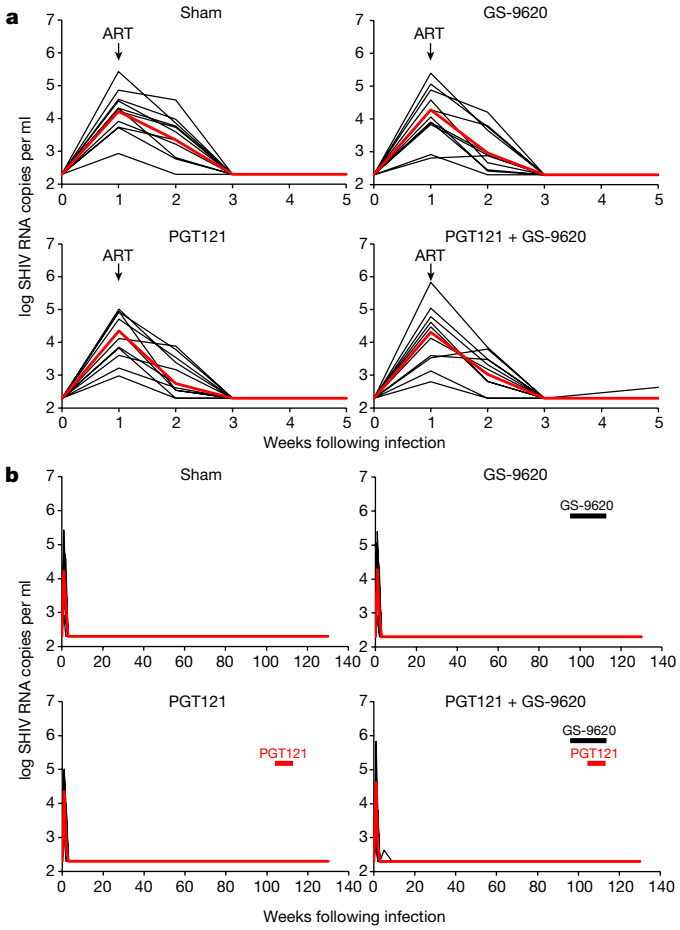

Fig. 1 | Plasma viral loads after infection with SHIV-SF162P3 and before discontinuation of ART. We infected 44 rhesus monkeys with SHIV-SF162P3 at week 0 and initiated ART at week 1 (day 7) ($n = 11$ monkeys per group). Administration of GS-9620 and infusions of PGT121 were performed from weeks 96 to 114. ART was discontinued at week 130. Plasma viral loads are shown for weeks 0–5 (**a**) and weeks 0–130 (**b**). Data are shown as log SIV RNA copies per ml (limit of detection 2.3 log RNA copies per ml). Red lines indicate median values.

antibody in monkeys[10]. Serum PGT121 declined to undetectable levels ($<0.5\ \mu g\ ml^{-1}$) in most monkeys by week 120 and in all monkeys by week 122 (Extended Data Fig. 4a). PGT121 was also undetectable in cell lysates and supernatants from lymph nodes and colorectal biopsies from week 120 (Extended Data Fig. 4b). We previously defined a PGT121 level of $1\ \mu g\ ml^{-1}$ as the threshold for viral rebound in SHIV-SF162P3-infected rhesus monkeys for PGT121-mediated virologic suppression[10]. Thus, PGT121 levels were below this rebound threshold in peripheral blood and lymphoid and gastrointestinal tissues for 8–10 weeks before discontinuation of ART at week 130.

Viral DNA

Viral DNA was largely undetectable in PBMCs in all groups of monkeys at week 96 and week 120 using quantitative PCR with reverse transcription (RT–PCR) with a sensitivity of 3 DNA copies per 10^6 PBMCs[20] (Fig. 3a, b), presumably as a result of the early initiation and the extended duration of suppressive ART. We still detected viral DNA in lymph nodes in the majority of monkeys at week 96 before the interventions, consistent with previous findings in rhesus monkeys treated with ART during acute SIVmac251 infection[24]. Following the interventions at week 120, we observed similar levels of viral DNA in the sham and GS-9620-alone groups. By contrast, monkeys treated with PGT121 and GS-9620 had lower levels of viral DNA in lymph nodes than did sham controls at week 120 (Fig. 3b; $P = 0.004$, Mann–Whitney test). We were unable to detect cellular RNA in all groups, both at week 96 and at week 120 (data not shown). These data suggest that bNAb administration with innate immune stimulation may have reduced the viral reservoir in these monkeys.

Cellular immune responses

Monkeys showed low levels of Gag-, Env-, and Pol-specific cellular immune responses at week 4, and these responses waned by week 96 and week 120 (Extended Data Fig. 5), presumably reflecting a lack of antigen stimulation during the extended period of ART suppression. Multi-parameter intracellular cytokine staining at week 120 corroborated these findings and showed minimal to no detectable $CD8^+$ T cell responses in PBMCs in all groups of monkeys (Extended Data Fig. 6a). Lymph node $CD8^+$ T cell responses and follicular $CXCR5^+CD8^+$ T cell responses were also marginal in all groups (Extended Data Fig. 6b). In particular, Gag-, Env- and Pol-specific $CD8^+$ T cell responses in PBMCs and lymph nodes were not higher in monkeys that received PGT121 than in those that did not, suggesting that there was no 'vaccinal effect' following antibody administration in this study.

Viral rebound following ART discontinuation

At week 130, we discontinued ART in all monkeys and monitored plasma viral loads for 196 days to assess viral rebound (Fig. 4a). In the sham control group, 11 of 11 monkeys (100%) rebounded with high peak viral loads and moderate setpoint viral loads typical of SHIV-SF162P3 infection[20,21]. In the GS-9620-alone group, 10 of 11 monkeys (91%) rebounded, and in the PGT121-alone group, 9 of 11 monkeys (82%) rebounded. In the group treated with both PGT121 and GS-9620, however, only 6 of 11 monkeys (55%) rebounded by day 196 following ART discontinuation. The monkeys treated with PGT121 and GS-9620 that rebounded also showed a 2.6 log reduction in peak viral loads and a 1.5 log reduction in setpoint viral loads as compared with sham controls (Fig. 4b; $P < 0.001$, χ^2 test comparing total viral load AUC). All monkeys that rebounded generated robust Gag-, Env- and Pol-specific cellular immune responses following viral rebound, which probably contributed to post-rebound virologic control (Extended Data Fig. 7a).

The median time to viral rebound in the sham group and in the GS-9620-alone group was 21 days, whereas the median time to viral rebound in the group that received PGT121 and GS-9620 was 5.3-fold longer at 112 days (Fig. 5a). Overall, the group that received PGT121 and GS-9620 demonstrated significantly delayed viral rebound compared with the sham group, and the PGT121-alone group showed a detectable but more modest effect (Fig. 5a, b; $P = 0.0001$, Kruskall–Wallis test comparing all groups; $P < 0.001$, censored Poisson regression model comparing PGT121+GS-9620 versus sham, PGT121 alone versus sham, and PGT121+GS-9620 versus PGT121 alone). These findings demonstrate that treatment with PGT121 and GS-9620 was superior to PGT121 alone in delaying viral rebound following ART discontinuation.

Monkeys treated with PGT121 and GS-9620 that did not rebound by day 196 following ART discontinuation had lower peak pre-ART plasma viral loads at week 1 of infection than those that did rebound (Fig. 5c; $P = 0.03$, Mann–Whitney test). Moreover, pre-ART viral loads correlated inversely with time to rebound in this group (Fig. 5c; $P = 0.03$, $R = -0.62$, Spearman rank-correlation test). Similar trends were observed in the monkeys that did not rebound in the other groups (Extended Data Fig. 7b). These data suggest that the extent of viral exposure before ART initiation was a key determinant of the therapeutic efficacy of PGT121 and GS-9620, probably by limiting initial seeding of the viral reservoir.

Adoptive transfer and CD8 depletion studies

Current viral DNA assays are insufficiently sensitive to predict viral rebound following ART discontinuation, as shown by the rapid rebound in 100% of sham controls (Fig. 4a), despite the absence of detectable viral DNA in PBMCs and lymph nodes in a subset of these monkeys at week 120 (Fig. 3b). These findings are also consistent with clinical observations that have shown viral rebound even in patients

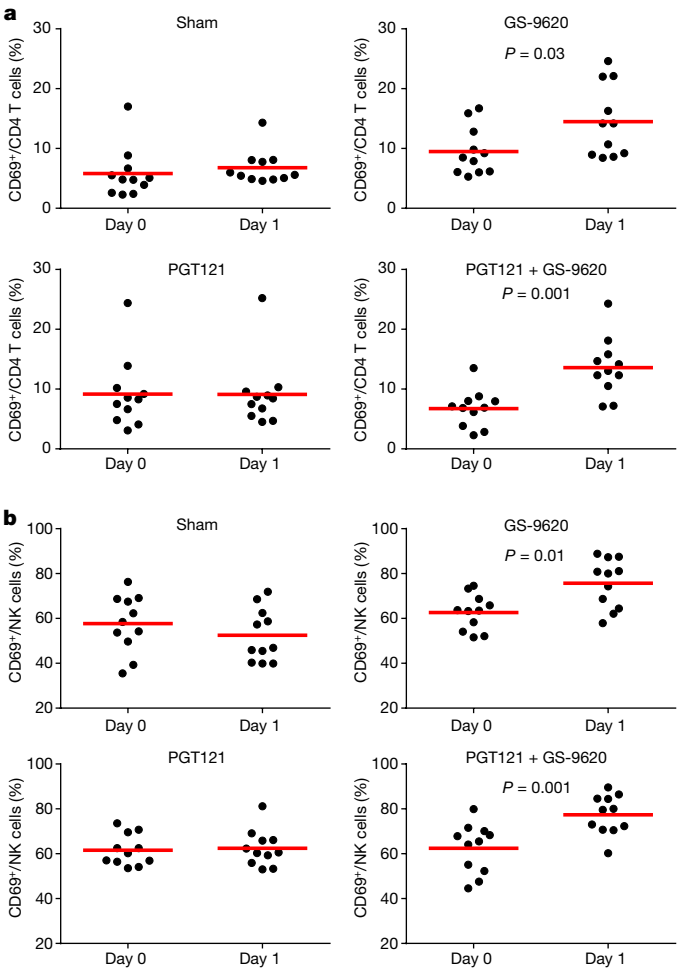

Fig. 2 | Cellular immune activation following administration of GS-9620 and before discontinuation of ART. Activation of $CD4^+$ T cells (**a**) and NK cells (**b**) was assessed by CD69 expression on days 0 and 1 after administration of GS-9620 ($n = 11$ monkeys per group). Representative data are shown following the fifth dose of GS-9620, which was comparable to the other doses. Red horizontal bars indicate median values. *P* values calculated using two-sided Mann–Whitney tests.

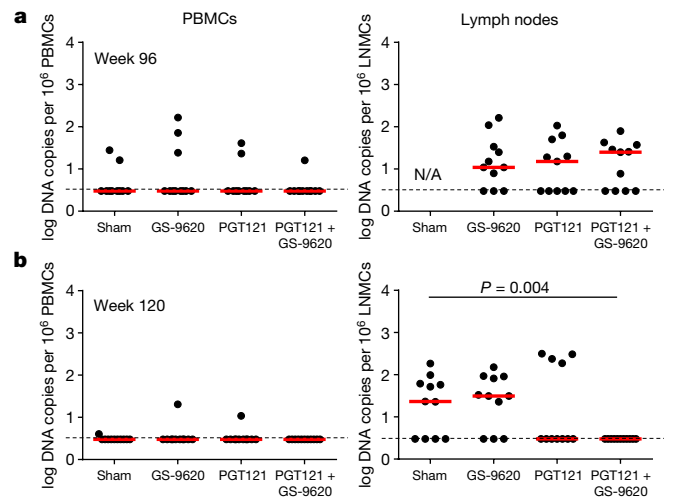

Fig. 3 | Viral DNA before discontinuation of ART. Data are shown as log viral DNA copies per 10^6 cells (limit of detection 3 DNA copies per 10^6 cells) in PBMCs and lymph node mononuclear cells (LNMCs) at week 96 before the interventions (**a**) and at week 120 following the interventions (**b**) ($n = 11$ monkeys per group). Red horizontal bars indicate median values. *P* values calculated using two-sided Mann–Whitney tests.

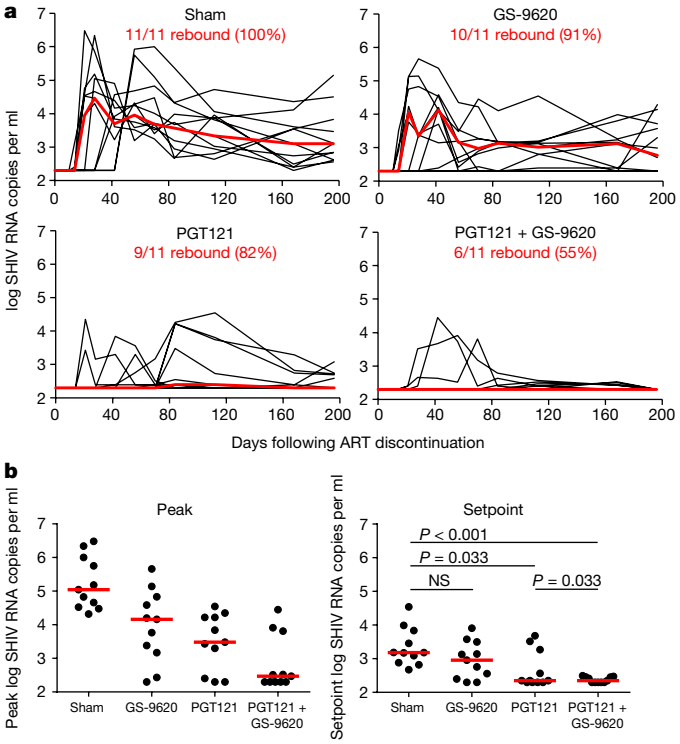

Fig. 4 | Viral loads following ART discontinuation. **a**, Plasma viral loads are shown for 196 days following ART discontinuation ($n = 11$ monkeys per group). Data are shown as log SIV RNA copies per ml (limit of detection 2.3 log RNA copies per ml). Numbers and percentages of monkeys that show viral rebound by day 196, defined as any confirmed detectable viral load, are shown. **b**, Summary of peak and setpoint viral loads following ART discontinuation ($n = 11$ monkeys per group). Red lines and horizontal bars indicate median values. *P* values calculated using χ^2 tests of area under the curve (AUC) total viral RNA following discontinuation of ART. NS, not significant.

with undetectable levels of viral DNA[25,26]. To assess residual replication-competent virus, we first performed an adoptive transfer study using PBMCs and lymph node mononuclear cells (LNMCs) from five of the seven monkeys that did not rebound and for which we had sufficient LNMCs available from day 140 following ART discontinuation, including four of the five monkeys treated with PGT121 and GS-9620 and one of the two monkeys treated with PGT121 alone. We infused 30 million PBMCs and LNMCs from these five monkeys by intravenous infusion into naive rhesus monkeys, and we used a similar number of PBMCs and LNMCs from two monkeys treated with PGT121 and GS-9620 that showed transient rebound followed by virologic control as positive controls. All monkeys had undetectable plasma viral RNA on day 140 when PBMCs and LNMCs were collected. Adoptive transfer of cells from the two monkeys that rebounded led to efficient infection of the naive hosts, as shown by high plasma viral loads of 6.1–6.8 log RNA copies per ml in recipients by day 14–21 following adoptive transfer (Fig. 6a, red lines). These data show that replication-competent virus persisted in these two monkeys despite post-rebound virologic control. By contrast, adoptive transfer of cells from the five monkeys that did not rebound failed to transfer infection to naive hosts (Fig. 6a, black lines).

We next depleted $CD8^+$ T cells and NK cells in the monkeys treated with PGT121 and GS-9620 that had undetectable viral loads on day 196 following ART discontinuation. Monkeys received a single intravenous infusion of 50 mg kg^{-1} of the anti-CD8α CDR-grafted rhesus IgG1 antibody MT807R1 (provided by K. Reimann, MassBiologics). Following infusion, all monkeys showed marked CD8 depletion in PBMCs (Extended Data Fig. 8) as well as in lymph nodes and colorectal biopsies (data not shown). In all the monkeys treated with PGT121 and GS-9620 that rebounded following ART discontinuation, plasma

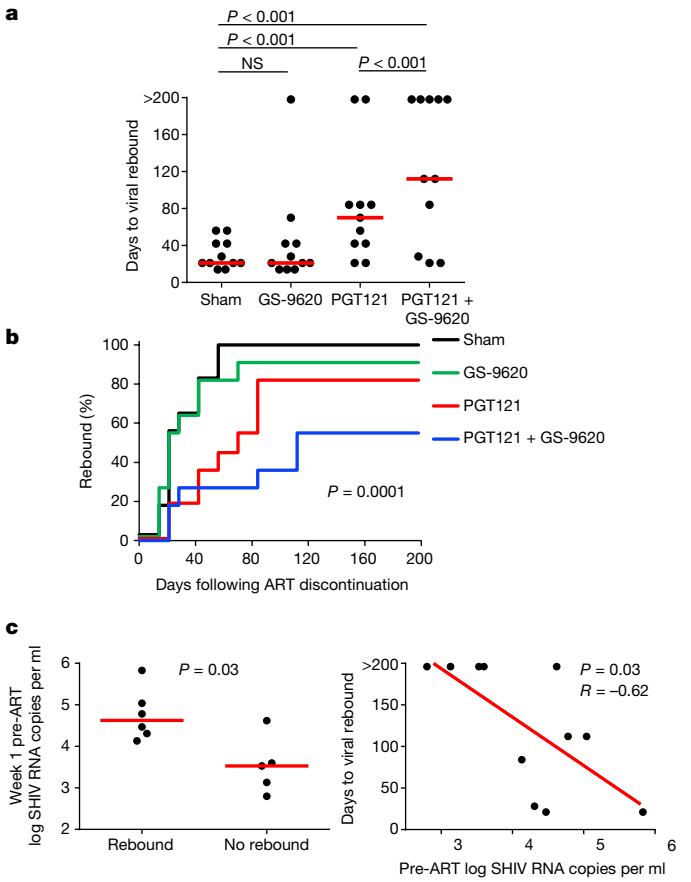

Fig. 5 | Analysis and correlations of viral rebound. a, **b**, Comparison of time to viral rebound among groups as dot plots depicting raw data (**a**) and Kaplan–Meier curves (**b**) ($n = 11$ monkeys per group). **c**, Correlation of viral rebound in monkeys treated with PGT121 and GS-9620 with pre-ART week 1 log viral RNA copies per ml ($n = 11$). Red horizontal bars indicate median values. *P* values calculated using a censored Poisson regression model of incidence rate ratios (**a**), a Kruskall–Wallis test (**b**), and a two-sided Spearman rank-correlation test (**c**).

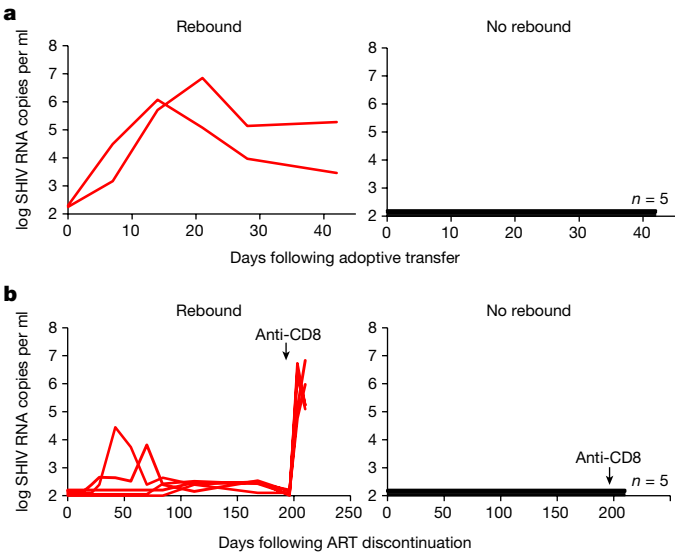

Fig. 6 | Adoptive transfer and CD8 depletion studies. a, Plasma viral loads in recipient monkeys following adoptive transfer of 30 million PBMCs and LNMCs from monkeys treated with PGT121 and GS-9620 that exhibited viral rebound and post-rebound virologic control ($n = 2$, left, red lines) and monkeys treated with PGT121 and GS-9620 or PGT121 alone that exhibited no viral rebound following discontinuation of ART ($n = 5$, which represents 4 from the PGT121 + GS-9620 group and 1 from the PGT121-alone group, right, black lines). **b**, Plasma viral loads in monkeys treated with PGT121 and GS-9620 before and after CD8 depletion (see Methods) in monkeys that exhibited viral rebound ($n = 5$, left, red lines) and in monkeys that exhibited no viral rebound following discontinuation of ART ($n = 5$, right, black lines). CD8 depletion was performed on day 196 (arrows).

viral loads spiked to 6.0–6.8 log RNA copies per ml by day 7–14 after CD8 depletion (Fig. 6b, red lines). By contrast, in the five monkeys that were treated with PGT121 and GS-9620 and did not rebound following ART discontinuation, viral loads remained undetectable following CD8 depletion (Fig. 6b, black lines).

Mechanistic studies

We developed a computational model that included cellular activation, innate plasma cytokines, and adaptive immune responses to define the correlates of delayed viral rebound in this study. A model that included NK cell activation correlated best with delayed viral rebound (Extended Data Fig. 9a; $P = 5.31 \times 10^{-4}$, $R = 0.50$, Spearman rank-correlation test). A similar model involving NK cell and monocyte activation correlated with reduced viral loads following ART discontinuation (Extended Data Fig. 9b; $P = 3.52 \times 10^{-6}$, $R = 0.64$, Spearman rank-correlation test). These data suggest that activated NK cells and monocytes may have a key role in PGT121-mediated elimination of infected $CD4^+$ T cells, consistent with the observed NK cell activation following GS-9620 activation (Fig. 2b).

Finally, we assessed the ability of PGT121, with or without GS-9620, to kill HIV-1-infected $CD4^+$ T cells in vitro. GS-9620 led to activation of NK cells and T cells in vitro (Extended Data Fig. 10a), consistent with the in vivo data (Fig. 2, Extended Data Fig. 2). Moreover, the combination of PGT121 and GS-9620 led to optimal killing of HIV-1-infected $CD4^+$ T cells in vitro (Extended Data Fig. 10b), consistent with previous studies[19]. Together, these data suggest a mechanism by which the TLR7 agonist GS-9620 stimulated innate immunity and activated multiple immune cell subsets in vivo including infected $CD4^+$ T cells (Fig. 2, Extended Data Fig. 2), rendering them more susceptible to PGT121-mediated recognition, as well as effector cells such as NK cells and monocytes (Fig. 2b, Extended Data Fig. 9), which may have facilitated PGT121-mediated elimination of these infected $CD4^+$ T cells.

Discussion

Our data demonstrate that PGT121 together with the TLR7 agonist vesatolimod (GS-9620) delayed viral rebound following discontinuation of ART in acutely treated, SHIV-SF162P3-infected rhesus monkeys. Moreover, five of eleven monkeys that were treated with PGT121 and GS-9620 showed no viral rebound for more than 6 months after cessation of ART and also did not reveal virus by highly sensitive adoptive transfer and CD8 depletion studies. This proof-of-concept study suggests that bNAb administration combined with innate immune stimulation may represent a potential strategy to target the viral reservoir.

Our findings extend previous observations that HIV-1-specific bNAbs have direct antiviral activity in SHIV-infected rhesus monkeys[10–12] and in HIV-1-infected humans[13–16]. However, these previous studies did not assess the potential of bNAbs to target the viral reservoir, which would require bNAbs to be administered during ART suppression and no longer be present at therapeutic levels following discontinuation of ART. We previously defined a PGT121 level of 1 μg ml^{-1} as the threshold for viral rebound in SHIV-SF162P3-infected rhesus monkeys for PGT121-mediated virologic control[10]. In the present study, PGT121 levels were undetectable (below 0.5 μg ml^{-1}) in peripheral blood, lymph nodes, and colorectal tissue for 8–10 weeks before discontinuation of ART (Extended Data Fig. 4). These findings suggest that the delayed viral rebound in monkeys treated with PGT121 and GS-9620 may reflect reservoir targeting rather than just direct antiviral activity.

The five monkeys in the PGT121- and GS-9620-treated group that showed sustained remission for more than 6 months following discontinuation of ART also did not show evidence of virus in adoptive transfer and CD8 depletion studies (Fig. 6), which are sensitive tests for residual replication-competent virus. Viral rebound can occur in humans following extended periods of ART-free remission[25,26]. We therefore cannot exclude the possibility that exceedingly low levels of replication-competent virus may still exist in these monkeys. Nevertheless, there was a clear difference between the monkeys that rebounded and those that did not rebound in the adoptive transfer and CD8 depletion studies (Fig. 6).

We hypothesize that the mechanism of the observed effects of PGT121 and GS-9620 involves activation of multiple cell types by GS-9620 followed by efficient binding and elimination of virally infected $CD4^+$ T cells by PGT121. GS-9620 activated $CD4^+$ T cells and NK cells, both in vivo (Fig. 2, Extended Data Fig. 2) and in vitro (Extended Data Fig. 10), and activated NK cells and monocytes correlated with delayed viral rebound following ART discontinuation (Extended Data Fig. 9). These data suggest that GS-9620 may have activated latently infected $CD4^+$ T cells, possibly rendering them more susceptible to PGT121 binding, and effector cells such as NK cells and monocytes, which may have facilitated antibody-mediated elimination of the infected $CD4^+$ T cells. This proposed mechanism predicts that a longer duration of combined PGT121 and GS-9620 therapy might improve therapeutic efficacy. In monkeys treated with PGT121 and GS-9620, we did not detect evidence of a 'vaccinal effect' of increased autologous antigen-specific $CD8^+$ T cell responses following bNAb administration (Extended Data Figs. 5, 6), in contrast to a previous study that involved bNAb administration during acute SHIV infection[27].

In summary, our data show that bNAb administration combined with innate immune stimulation can delay viral rebound following discontinuation of ART. This study used rhesus monkeys in which ART was initiated on day 7 of acute infection and then received ART continuously for 2.5 years. Moreover, the maximum therapeutic effect was observed in monkeys with the lowest pre-ART viral loads (Fig. 5c). It will therefore probably be far more difficult to achieve similar results in monkeys in which ART is initiated during chronic infection, and thus implications for typical HIV-1-infected humans remain unclear. Nevertheless, our data provide an initial proof-of-concept in primates showing the potential of innate immune activation with immune-based targeting of the viral reservoir.

Online content

Any methods, additional references, Nature Research reporting summaries, source data, statements of data availability and associated accession codes are available at https://doi.org/10.1038/s41586-018-0600-6.

Received: 21 April 2018; Accepted: 14 September 2018;
Published online 3 October 2018.

1. Finzi, D. et al. Identification of a reservoir for HIV-1 in patients on highly active antiretroviral therapy. *Science* **278**, 1295–1300 (1997).
2. Persaud, D., Zhou, Y., Siliciano, J. M. & Siliciano, R. F. Latency in human immunodeficiency virus type 1 infection: no easy answers. *J. Virol.* **77**, 1659–1665 (2003).
3. Chun, T. W. et al. Presence of an inducible HIV-1 latent reservoir during highly active antiretroviral therapy. *Proc. Natl Acad. Sci. USA* **94**, 13193–13197 (1997).
4. Ho, Y. C. et al. Replication-competent noninduced proviruses in the latent reservoir increase barrier to HIV-1 cure. *Cell* **155**, 540–551 (2013).
5. Finzi, D. et al. Latent infection of CD4+ T cells provides a mechanism for lifelong persistence of HIV-1, even in patients on effective combination therapy. *Nat. Med.* **5**, 512–517 (1999).
6. Chun, T. W., Davey, R. T., Jr, Engel, D., Lane, H. C. & Fauci, A. S. Re-emergence of HIV after stopping therapy. *Nature* **401**, 874–875 (1999).
7. Barouch, D. H. & Deeks, S. G. Immunologic strategies for HIV-1 remission and eradication. *Science* **345**, 169–174 (2014).
8. Deeks, S. G. et al. International AIDS Society global scientific strategy: towards an HIV cure 2016. *Nat. Med.* **22**, 839–850 (2016).
9. Shan, L. et al. Stimulation of HIV-1-specific cytolytic T lymphocytes facilitates elimination of latent viral reservoir after virus reactivation. *Immunity* **36**, 491–501 (2012).
10. Barouch, D. H. et al. Therapeutic efficacy of potent neutralizing HIV-1-specific monoclonal antibodies in SHIV-infected rhesus monkeys. *Nature* **503**, 224–228 (2013).
11. Shingai, M. et al. Antibody-mediated immunotherapy of macaques chronically infected with SHIV suppresses viraemia. *Nature* **503**, 277–280 (2013).
12. Julg, B. et al. Virological control by the CD4-binding site antibody N6 in simian-human immunodeficiency virus-infected rhesus monkeys. *J. Virol.* **91**, e00498-17 (2017).
13. Caskey, M. et al. Viraemia suppressed in HIV-1-infected humans by broadly neutralizing antibody 3BNC117. *Nature* **522**, 487–491 (2015).
14. Caskey, M. et al. Antibody 10-1074 suppresses viremia in HIV-1-infected individuals. *Nat. Med.* **23**, 185–191 (2017).
15. Scheid, J. F. et al. HIV-1 antibody 3BNC117 suppresses viral rebound in humans during treatment interruption. *Nature* **535**, 556–560 (2016).
16. Bar, K. J. et al. Effect of HIV antibody VRC01 on viral rebound after treatment interruption. *N. Engl. J. Med.* **375**, 2037–2050 (2016).
17. Walker, L. M. et al. Broad neutralization coverage of HIV by multiple highly potent antibodies. *Nature* **477**, 466–470 (2011).
18. Liu, J. et al. Antibody-mediated protection against SHIV challenge includes systemic clearance of distal virus. *Science* **353**, 1045–1049 (2016).
19. Tsai, A. et al. Toll-like receptor 7 agonist GS-9620 induces HIV expression and HIV-specific immunity in cells from HIV-infected individuals on suppressive antiretroviral therapy. *J. Virol.* **91**, e02166-16 (2017).
20. Borducchi, E. N. et al. Ad26/MVA therapeutic vaccination with TLR7 stimulation in SIV-infected rhesus monkeys. *Nature* **540**, 284–287 (2016).
21. Barouch, D. H. et al. Protective efficacy of a global HIV-1 mosaic vaccine against heterologous SHIV challenges in rhesus monkeys. *Cell* **155**, 531–539 (2013).
22. Kawai, T. et al. Interferon-α induction through Toll-like receptors involves a direct interaction of IRF7 with MyD88 and TRAF6. *Nat. Immunol.* **5**, 1061–1068 (2004).
23. Hemmi, H. et al. Small anti-viral compounds activate immune cells via the TLR7 MyD88-dependent signaling pathway. *Nat. Immunol.* **3**, 196–200 (2002).
24. Whitney, J. B. et al. Rapid seeding of the viral reservoir prior to SIV viraemia in rhesus monkeys. *Nature* **512**, 74–77 (2014).
25. Henrich, T. J. et al. Antiretroviral-free HIV-1 remission and viral rebound after allogeneic stem cell transplantation: report of 2 cases. *Ann. Intern. Med.* **161**, 319–327 (2014).
26. Persaud, D. et al. Absence of detectable HIV-1 viremia after treatment cessation in an infant. *N. Engl. J. Med.* **369**, 1828–1835 (2013).
27. Nishimura, Y. et al. Early antibody therapy can induce long-lasting immunity to SHIV. *Nature* **543**, 559–563 (2017).

Acknowledgements We thank K. Reimann and A. Hill for advice, assistance, and reagents. We acknowledge support from the Bill & Melinda Gates Foundation (OPP1107669), the American Foundation for AIDS Research (109219-58-RGRL), the National Institutes of Health (AI096040, AI124377, AI126603, AI129797, AI128751, OD024917), and the Ragon Institute of MGH, MIT, and Harvard.

Author contributions D.H.B. and R.G. designed the study. J.H. and R.G. developed the ART formulation and TLR7 agonist. E.B. conducted the cytokine analyses. E.N.B., J.L., J.P.N., A.M.C., P.A., N.B.M., A.C., D.J., L.P., K.M., and E.T.M. performed the immunologic and virologic assays. W.-H.Y., S.F., T.B., and G.A. led the computational modelling. W.L. led the statistical analysis. M.G.L. led the clinical care of the rhesus monkeys. D.H.B. led the study and wrote the paper with all co-authors.

Competing interests E.B., J.H., and R.G. are employees of Gilead Sciences. The other authors declare no competing interests.

Additional information
Extended data is available for this paper at https://doi.org/10.1038/s41586-018-0600-6.
Supplementary information is available for this paper at https://doi.org/10.1038/s41586-018-0600-6.
Reprints and permissions information is available at http://www.nature.com/reprints.
Correspondence and requests for materials should be addressed to D.H.B.
Publisher's note: Springer Nature remains neutral with regard to jurisdictional claims in published maps and institutional affiliations.

METHODS

Monkeys and study design. Forty-four outbred Indian-origin, young adult male and female rhesus monkeys (*M. mulatta*) were genotyped, and animals that expressed protective MHC class I alleles and susceptible and resistant TRIM5α alleles were distributed among the groups. Each group had 0 *Mamu-A*01*, 1 or 2 *Mamu-B*17*, and 0 or 1 *Mamu-B*08* animals. Animals were otherwise randomly allocated to groups. All monkeys were housed at Bioqual, Rockville, MD. Animals were infected with a single 500 $TCID_{50}$ dose of our rhesus PBMC-derived SHIV-SF162P3 challenge stock[21] by the intrarectal route. ART was initiated on day 7. Monkeys were bled up to twice per week for viral load determinations. Monkeys received the following interventions starting at week 96 ($n = 11$/group): (1) sham controls, (2) vesatolimod (GS-9620) alone, (3) PGT121 alone, or (4) both (Extended Data Fig. 1). In groups 2 and 4, animals received 10 oral administrations of 0.15 mg/kg GS-9620 (Gilead Sciences, Foster City, CA) every 2 weeks from weeks 96 to 114. In Groups 3 and 4, animals received 5 intravenous infusions of 10 mg/kg PGT121 (Catalent Biopharma, Madison, WI) every 2 weeks from weeks 106 to 114. Cytokine levels were determined by Luminex assays, and T cell and NK cell activation was assessed by multiparameter flow cytometry. Immunologic and virologic assays were performed blinded. ART was discontinued at week 130. All animal studies complied with all relevant ethical regulations and were approved by the Bioqual Institutional Animal Care and Use Committee (IACUC).

ART regimen. The formulated antiretroviral therapy (ART) cocktail contained 5.1 mg/ml tenofovir disoproxil fumarate (TDF), 40 mg/ml emtricitabine (FTC), and 2.5 mg/ml dolutegravir (DTG) in water containing 15% (v/v) kleptose adjusted to pH 4.2. This ART cocktail was administered once daily at 1 ml/kg body weight via the subcutaneous route.

Adoptive transfer studies. For adoptive transfer studies, 30 million LNMCs and PBMCs from PGT121+GS-9620- or PGT121-treated animals, collected on day 140 following ART discontinuation, were infused intravenously into healthy, SHIV-uninfected rhesus monkeys. Viral loads were assessed in recipient animals weekly following adoptive transfer.

CD8 depletion studies. For CD8 depletion studies, animals received a single intravenous infusion of 50 mg/kg of the anti-CD8α CDR-grafted rhesus IgG1 antibody MT807R1 (Keith Reimann, MassBiologics, Mattapan, MA). CD8 T cell counts and viral loads were assessed weekly following anti-CD8 infusion.

PGT121 pharmacokinetics. ImmunoClear ELISA plates (Thermo Scientific) were coated with 100 ng/well clade C (C97ZA.012) gp140 Env protein capture reagent overnight at 4 °C. Plates were then washed with PBS–0.05% Tween 20 and blocked for 2 h at room temperature with Blocker Casein in PBS (Pierce). Standard curve calibrators and diluted serum samples were incubated on the plates for 1 h before further washing and subsequent incubation with a mouse PGT121 anti-idiotype (1 μg/ml) monoclonal antibody. Plates were washed again and then incubated with 1:1,000 dilution of rabbit anti-mouse IgG-horseradish peroxidase (Thermo Scientific). Finally, plates were washed and developed for 5 min using SureBlue (KPL Laboratories) followed by addition of TMB Stop solution (KPL Laboratories). Plates were read at 450 nm on a VersaMax microplate reader (Molecular Devices) using Softmax Pro version 6.5.1 software. The SoftMax Pro software calculated 4-Parameter Logistic (4-PL) curve fits for the standard calibrators and the test sample concentrations were determined by interpolation into the calibration curves.

PGT121 anti-drug antibody (ADA) assays. ADA assays were performed using the MesoScale Discovery (MSD) electrochemiluminescence (ECL) platform. In brief, serum samples were diluted in assay buffer and incubated with a master mix containing sulfo-tagged and biotinylated-tagged PGT121 (at equimolar concentrations of 0.5 μg/ml) overnight at 4 °C on an orbital plate shaker. The mixture was then incubated on a streptavidin-functionalized plate and washed, and tripropylamine (TPA) was added and read using an MSD SQ-120 ECL imager. Luminescence was proportional to the amount of ADA. The assay positivity cut-point was defined as the 95th percentile of ECL signal response observed using naive NHP serum samples.

Cellular immune assays. SIV-specific cellular immune responses were assessed using IFN-γ ELISPOT assays and multiparameter intracellular cytokine staining (ICS) assays essentially as described[20]. ICS assays were performed with 10^6 PBMCs or LNMCs that were incubated for 6 h at 37 °C with medium, 10 pg/ml phorbol myristate acetate (PMA) and 1 μg/ml ionomycin (Sigma-Aldrich), or 1 μg/ml HIV-1 Env, SIV Gag, or SIV Pol peptide pools. Cultures contained monensin (GolgiStop; BD Biosciences), brefeldin A (GolgiPlug; BD Biosciences), and 1 μg/ml of a mAb against human CD49d (clone 9F10). Cells were then stained with predetermined titres of mAbs against CD3 (clone SP34.2;, Alexa 700), CD4 (clone L200; BV786), CD8 (clone SK1; APC H7), CD28 (clone L293, PerCP-Cy5.5), CD95 (clone DX2, BV711), CD20 (clone 2H10, BV570), CCR5 (clone 3A9, PE), BCL6 (clone K112-91, PE-CF594), CXCR5 (clone MU5UBEE, PE-cy7), and PD-1 (clone EH12.2H7, Pacific Blue); and stained intracellularly with IFN-γ (clone B27; BUV395), IL-2 (clone MQ1-17H12; BUV737), TNF-α (clone Mab11; BV650), CD69 (clone FN50, BV510), and Ki67 (clone B56, FITC). IFN-γ backgrounds were <0.05% in PBMCs.

Viral RNA assays. Viral RNA was isolated from cell-free plasma using a viral RNA extraction kit (Qiagen) and was quantified essentially as described[24].

Viral DNA assays. Levels of proviral DNA were quantified as previously described[24]. Total cellular DNA was isolated from 5×10^6 cells using a QIAamp DNA Blood Mini kit (Qiagen). The absolute quantification of viral DNA in each sample was determined by qPCR using primers specific to a conserved region SIVmac239. All samples were directly compared to a linear virus standard and the simultaneous amplification of a fragment of human GAPDH gene. PCR assays were performed with 100–200 ng sample DNA.

Computational modelling. The frequencies of cell populations at week 106 (corresponding to the sixth GS-9620 administration) before and after the intervention were used for the computational model. Z-score standardization was performed to have all features mean centred and unit variance scaled. The minimal correlates that best predicted viral rebound (or total viral loads) were identified by using a two-step model: least absolute shrinkage and selection operator (LASSO) regularization followed by partial least squares regression analysis (PLSR). The LASSO method was used to remove irrelevant features in order to improve the robustness of high-dimensional modelling. Next, PLSR was used to model the covariance relationship between the feature variables (X) and the outcome variables (Y), in the way that PLSR decomposes both X and Y into a hyperplane and maximizes covariance between the hyperplanes. To estimate the minimal correlates that best explain the outcome without overfitting, 5,000 repeated fivefold nested cross-validation was designed. In each repetition, the data set was randomly divided into five folds, where 80% of the data set was used for building the model and the remaining holdout set was used to test the model prediction, where the goodness-of-fitness of the model was measured by mean squared error (MSE) between prediction and the outcome. This approach resulted in the generation of a model with the minimal set of the features that generates the best outcome prediction in cross-validation test. In addition, variable importance in projection (VIP), a weighted sum of squares of the PLSR weights that summarized the importance of the features in a PLSR model with multiple components, was computed. To estimate the statistical significance of the optimized model with the defined correlates, we employed two types of permutation tests (shuffling the outcome label and selecting the randomized correlates) to test the likelihood of obtaining a model prediction accuracy by chance. Each permutation test performed 1,000 times to generate an empirical null distribution, and an exact P value of the model was computed.

PGT121-mediated $CD4^+$ T cell killing assay. Human PBMCs were isolated from fresh blood from healthy donors using SepMate PBMC Isolation tubes (StemCell Technologies) and histopaque (Sigma Aldrich) according to the manufacturer's protocol. Using an aliquot of PBMCs, $CD4^+$ T cells were isolated for HIV-1 infection using the EasySep Human $CD4^+$ T Cell Isolation Kit (StemCell Technologies). Remaining PBMCs were treated with 1,000 nM GS-9620 or DMSO and cultured at 3.0×10^6 cells/ml for 5 days in RPMI 1640 (Sigma Aldrich) medium supplemented with L-glutamine, HEPES, and IL-15 (1 ng/ml) at 37 °C. For HIV-1 infection, freshly isolated $CD4^+$ T cells were spinfected for 45 min at 1,500 RPM with NL4-3 virus (or medium for mock infection) and then treated with CD3/CD28 Human T Activator Dynabeads (ThermoFisher Scientific). Infected $CD4^+$ T cells were subsequently cultured for 5 days in R10 and IL-2 (30 units/ml) at 37 °C. Cells were counted daily and supplemented with fresh medium with IL-2 as needed. On day 5, both sets of cells were counted, washed twice and resuspended in fresh medium. HIV-infected $CD4^+$ T cells were incubated with 10 μg/ml of PGT121 for 30 min. Co-cultures of infected $CD4^+$ T cells and autologous donor PBMCs were then set up at a ratio of 1:10 (5.0×10^4 $CD4^+$ T cells; 5.0×10^5 PBMCs) and incubated overnight in R10 and IL-2 at 37 °C. Following the overnight incubation, cells were stained with Fixable Aqua viability dye (Invitrogen) followed by surface staining with CD4-APC (Invitrogen), CD56-PE-Cy7 (BD), CD3-AF700 (BD), and CD69-BV605 (BD). Cells were fixed and permeabilized with Cytofix/Cytoperm (BD Biosciences) and stained intracellularly with anti-KC57-PE-labelled p24 antibody (Beckman Coulter) in 1× Perm/Wash Buffer (BD Biosciences, 554723). Gating on viable $CD3^+CD4^+p24^+$ T cells was used to evaluate viral killing with each treatment condition normalized to an uninfected control. Per cent killing was normalized to the untreated antibody condition.

Statistical analyses. Analysis of virologic and immunologic data was performed using GraphPad Prism v6.03 (GraphPad Software). Comparisons of groups was performed using two-sided Mann–Whitney tests without Bonferroni adjustments. Correlations were assessed by two-sided Spearman rank-correlation tests. Analysis of viral rebound was performed using Kruskall–Wallis tests to compare all groups. For group pairwise comparisons, area under the curve (AUC) for total viral RNA following ART discontinuation was compared with chi-square tests, and viral rebound was compared with a censored Poisson regression model. In vitro killing data were analysed with paired Student's t-tests.

No statistical methods were used to predetermine sample size. Except as stated, the experiments were not randomized, and investigators were not blinded to allocation during experiments and outcome assessment.

Reporting summary. Further information on experimental design is available in the Nature Research Reporting Summary linked to this paper.

Data availability

All data generated and analysed in this study are available from the corresponding author upon reasonable request. Source data for figures from individual animals are available online.

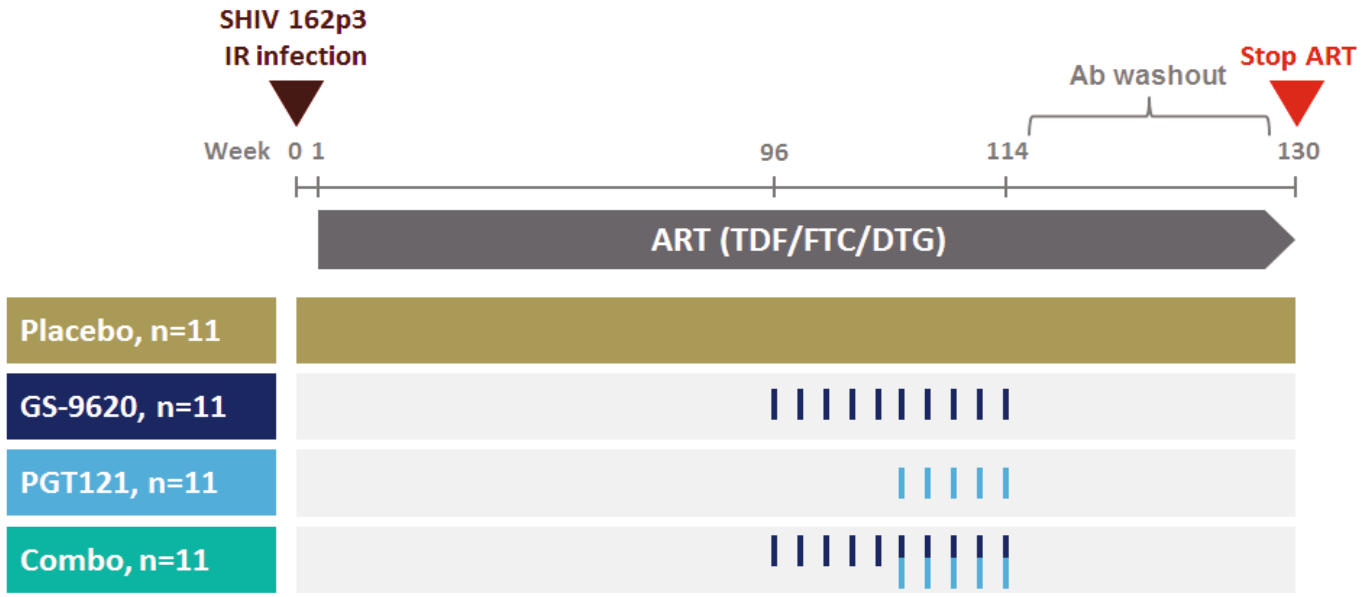

Extended Data Fig. 1 | Study design. Forty-four rhesus monkeys ($n = 11$ monkeys per group) were infected with SHIV-SF162P3 at week 0 and ART was initiated at week 1 (day 7). GS-9620 administrations and PGT121 infusions are shown from weeks 96 to 114. ART was discontinued at week 130.

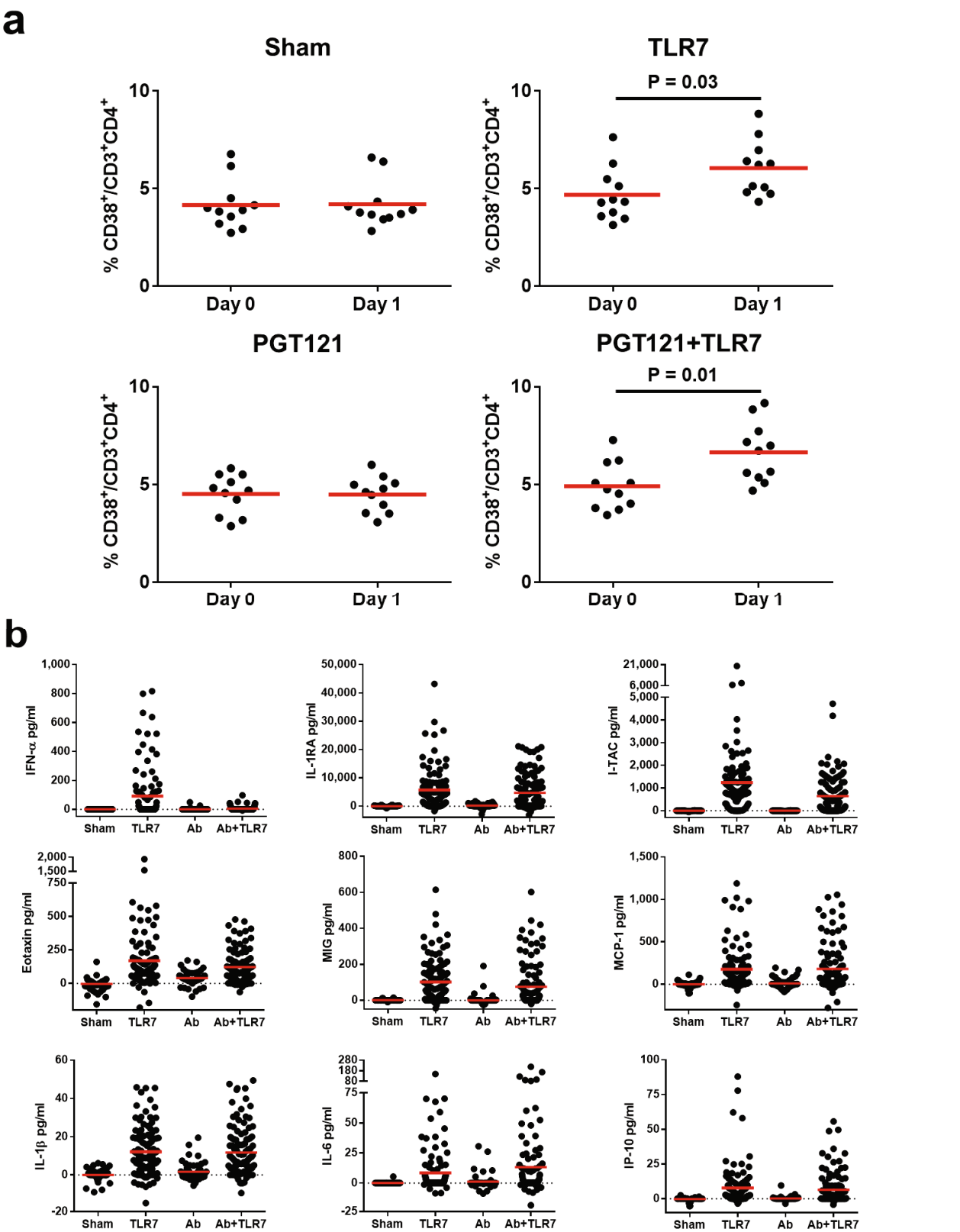

Extended Data Fig. 2 | Immune activation following GS-9620 administration and before ART discontinuation. a, Activation of $CD4^+$ T cells was assessed by CD38 expression on days 0 and 1 following GS-9620 administration, supplementing the data shown in Fig. 2a ($n = 11$ monkeys per group). Representative data are shown following the fifth GS-9620 dose, which was comparable to the other doses. Red horizontal bars indicate median values. *P* values reflect two-sided Mann–Whitney tests. **b**, Plasma levels of IFNα, IL-1RA, I-TAC, eotaxin, MIG, MCP-1, IL-1β, IL-6, IP-10 are shown on day 1 following GS-9620 administration ($n = 11$ monkeys per group). Red bars represent mean values. Combined data from all GS-9620 administrations with pre-dose levels subtracted are shown.

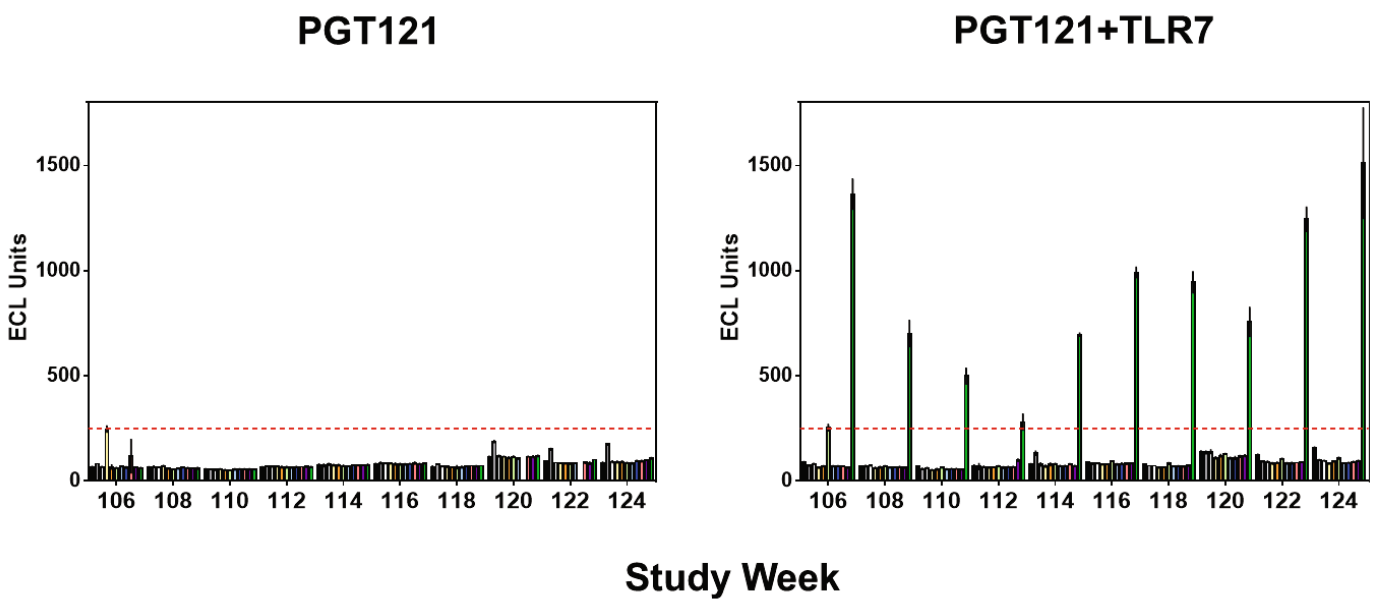

Extended Data Fig. 3 | Anti-drug antibody (ADA) assay before ART discontinuation. ADA responses were assessed in the PGT121+GS-9620 and PGT121-alone groups every 2 weeks from weeks 106 to 124 using an electrochemoluminescence (ECL) assay with an anti-PGT121 idiotypic mAb ($n = 11$ monkeys per group). No ADA was detected. One monkey in the PGT121+GS-9620 group had background reactivity in this assay at week 106 before PGT121 exposure (green bars).

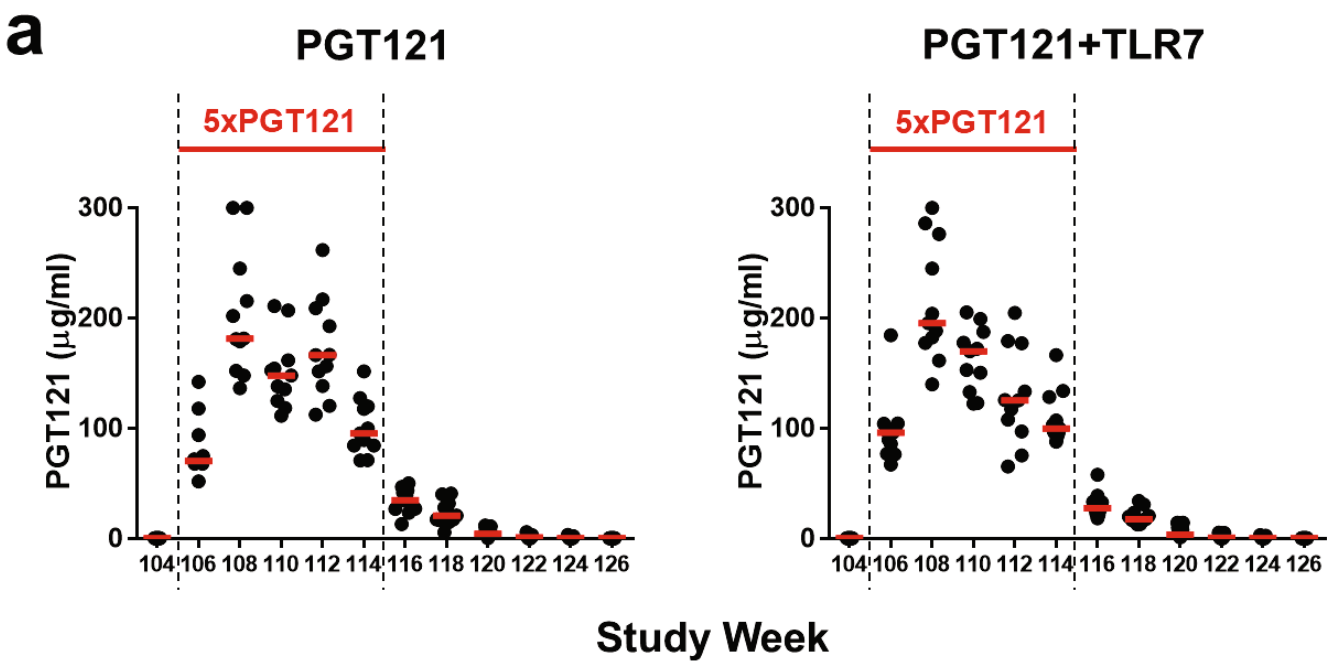

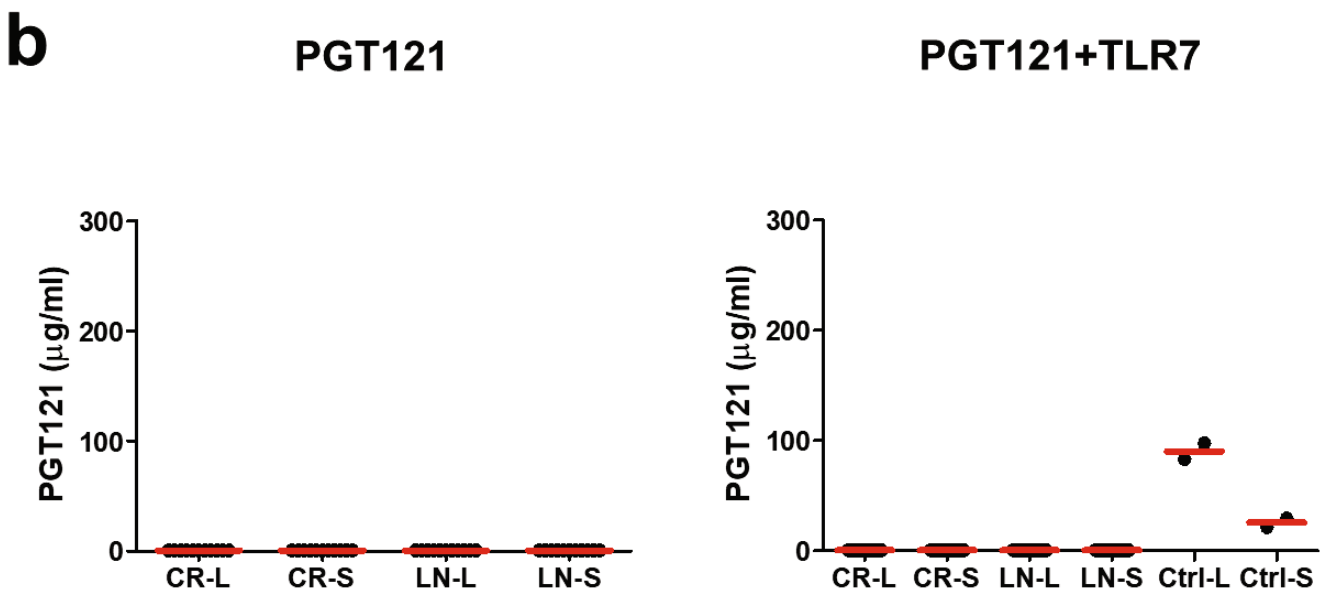

Extended Data Fig. 4 | PGT121 pharmacokinetics in serum and tissues before ART discontinuation. a, Peak serum PGT121 levels are shown (limit of detection 0.5 μg ml^{-1}) 1 h following each of five infusions of PGT121 (weeks 106–114) and during the washout period (weeks 114–130) ($n = 11$ monkeys per group). **b**, PGT121 levels (limit of detection 0.5 μg ml^{-1}) were assessed in cell lysates (L) and initial wash supernatants (S) from 10^6 lymph node (LN) and colorectal (CR) cells from week 120 ($n = 11$ monkeys per group). Positive controls (Ctrl) included lymph node samples from naive monkeys spiked with PGT121. Red bars represent median values.

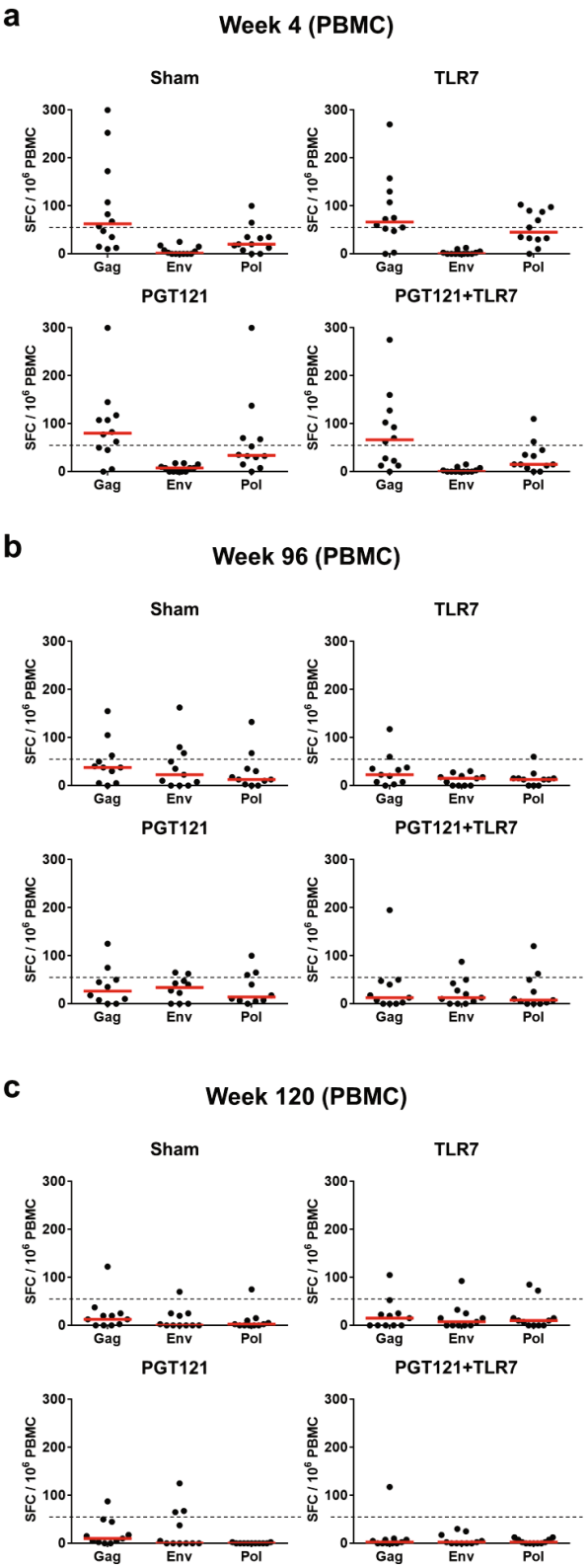

Extended Data Fig. 5 | IFNγ ELISPOT responses before ART discontinuation. Gag-, Env-, and Pol-specific IFNγ ELISPOT responses in PBMCs are shown at week 4 (**a**), week 96 (**b**), and week 120 (**c**) ($n = 11$ monkeys per group). Spot-forming cells (SFCs) per million PBMCs are shown. Red horizontal bars indicate median values. The dotted line represents the assay limit of quantitation (55 SFCs per million PBMCs).

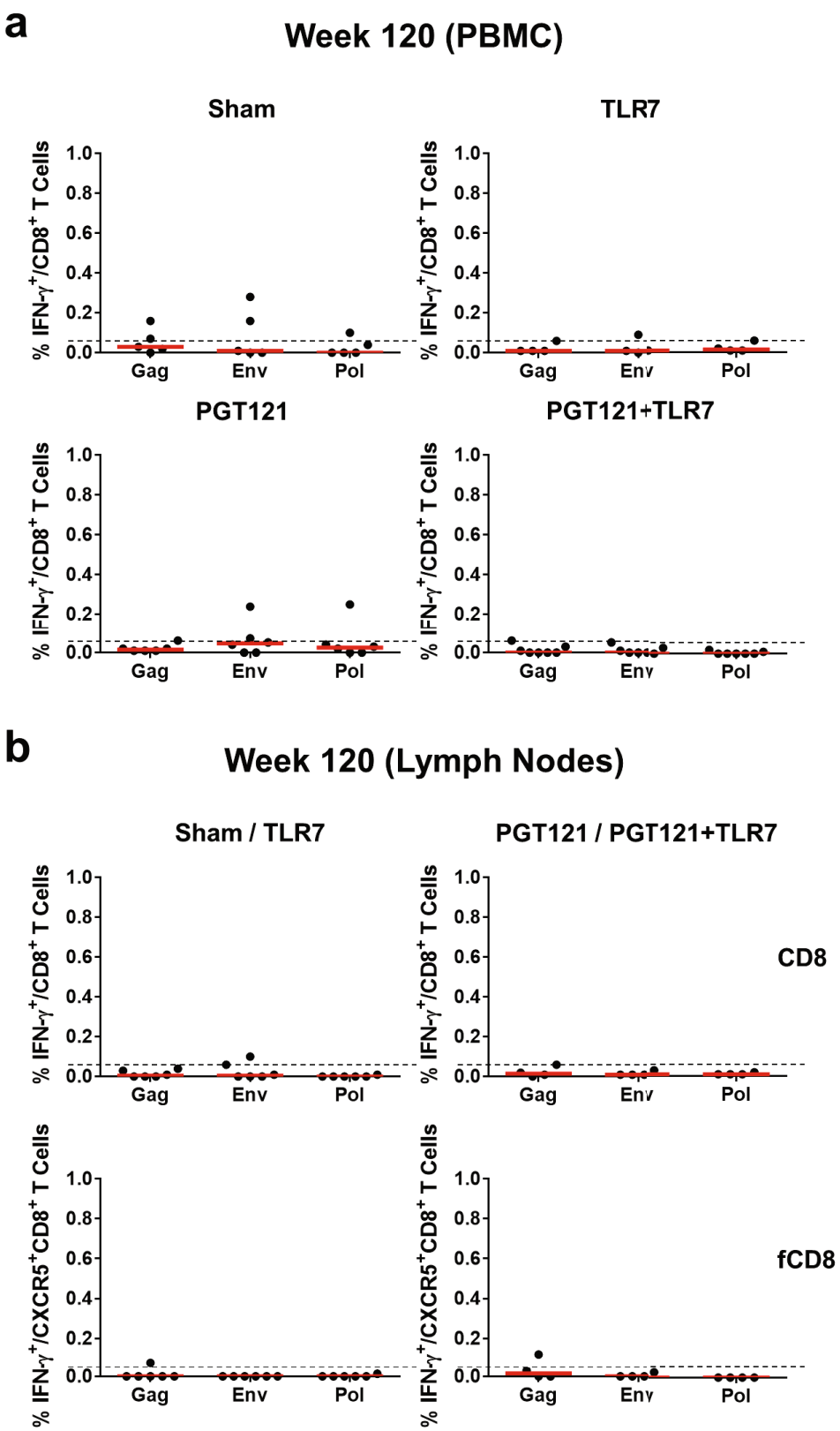

Extended Data Fig. 6 | IFNγ intracellular cytokine staining (ICS) responses before ART discontinuation. Gag-, Env-, and Pol-specific IFNγ ICS responses in PBMCs (**a**) and in LNMCs (**b**) are shown at week 120 ($n = 11$ monkeys per group). Per cent IFNγ-producing $CD8^+CD3^+$ T cells in PBMCs and per cent IFNγ-producing total $CD8^+CD3^+$ T cells (CD8) and follicular $CXCR5^+CD8^+CD3^+$ T cells (fCD8) in LNMCs are shown. Red horizontal bars indicate median values. The dotted line represents the assay limit of quantitation (0.05% $CD8^+CD3^+$ T cells).

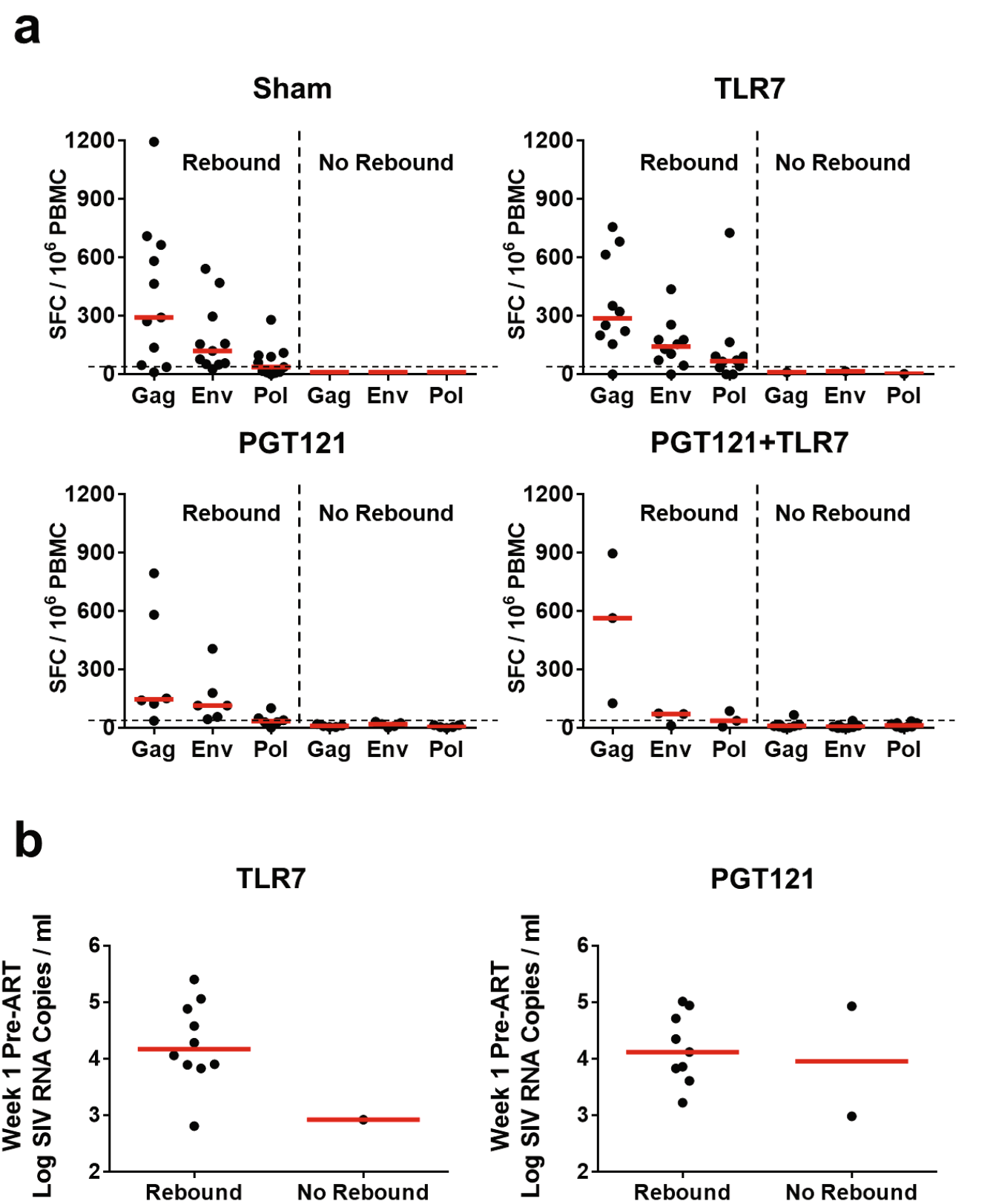

Extended Data Fig. 7 | IFNγ ELISPOT responses following ART discontinuation and trends for viral rebound. a, Gag-, Env-, and Pol-specific IFNγ ELISPOT responses in PBMCs are shown at day 140 following ART discontinuation ($n = 11$ monkeys per group). SFCs per million PBMCs are shown. Monkeys in each group that demonstrated viral rebound versus no rebound are shown separately. Red horizontal bars indicate median values. The dotted line represents the assay limit of quantitation (55 SFCs per million PBMCs). **b**, Trends for viral rebound are shown in the GS-9620 and PGT121 groups in relation to pre-ART week 1 viral loads, supplementing the data shown in Fig. 5c. Red horizontal bars indicate median values.

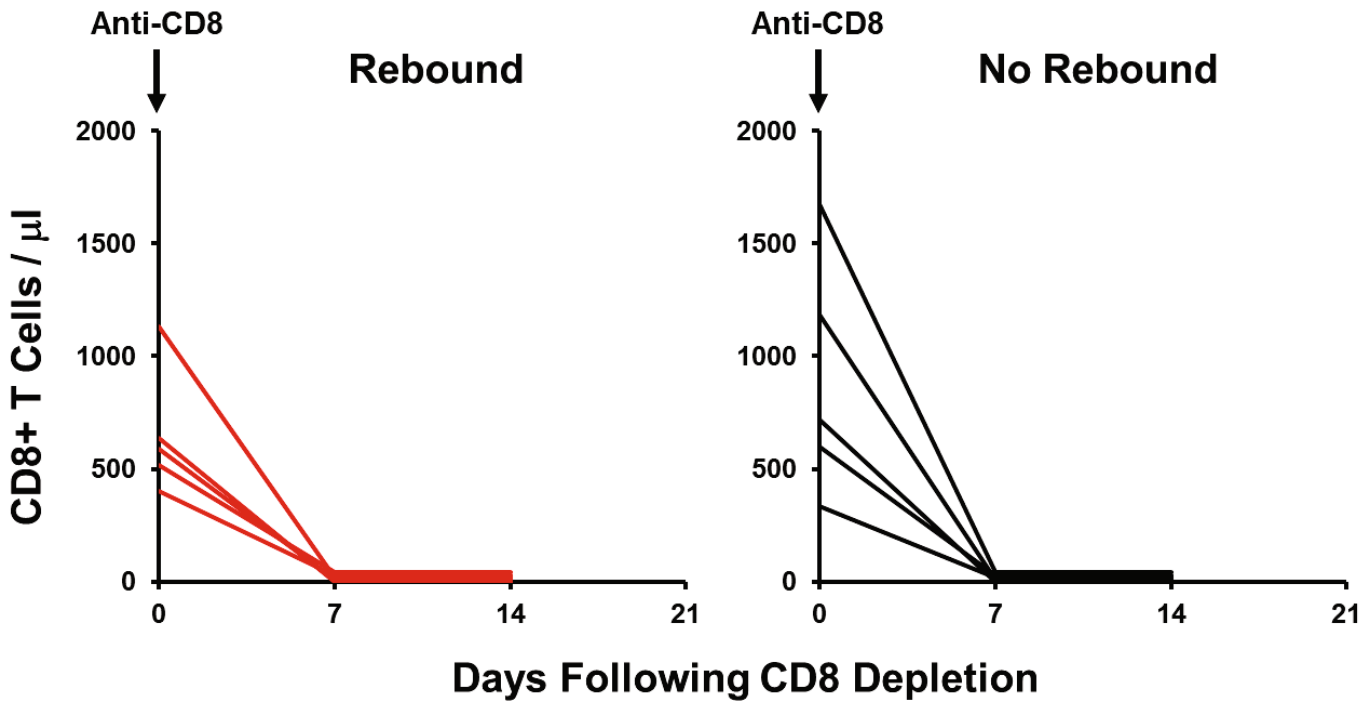

Extended Data Fig. 8 | CD8 depletion efficiency. $CD8^+$ T cells per µl peripheral blood are shown in PGT121+GS-9620-treated monkeys before and after CD8 depletion in monkeys that exhibited viral rebound and post-rebound virologic control ($n = 5$, left, red lines) and in monkeys that exhibited no viral rebound following ART discontinuation ($n = 5$, right, black lines).

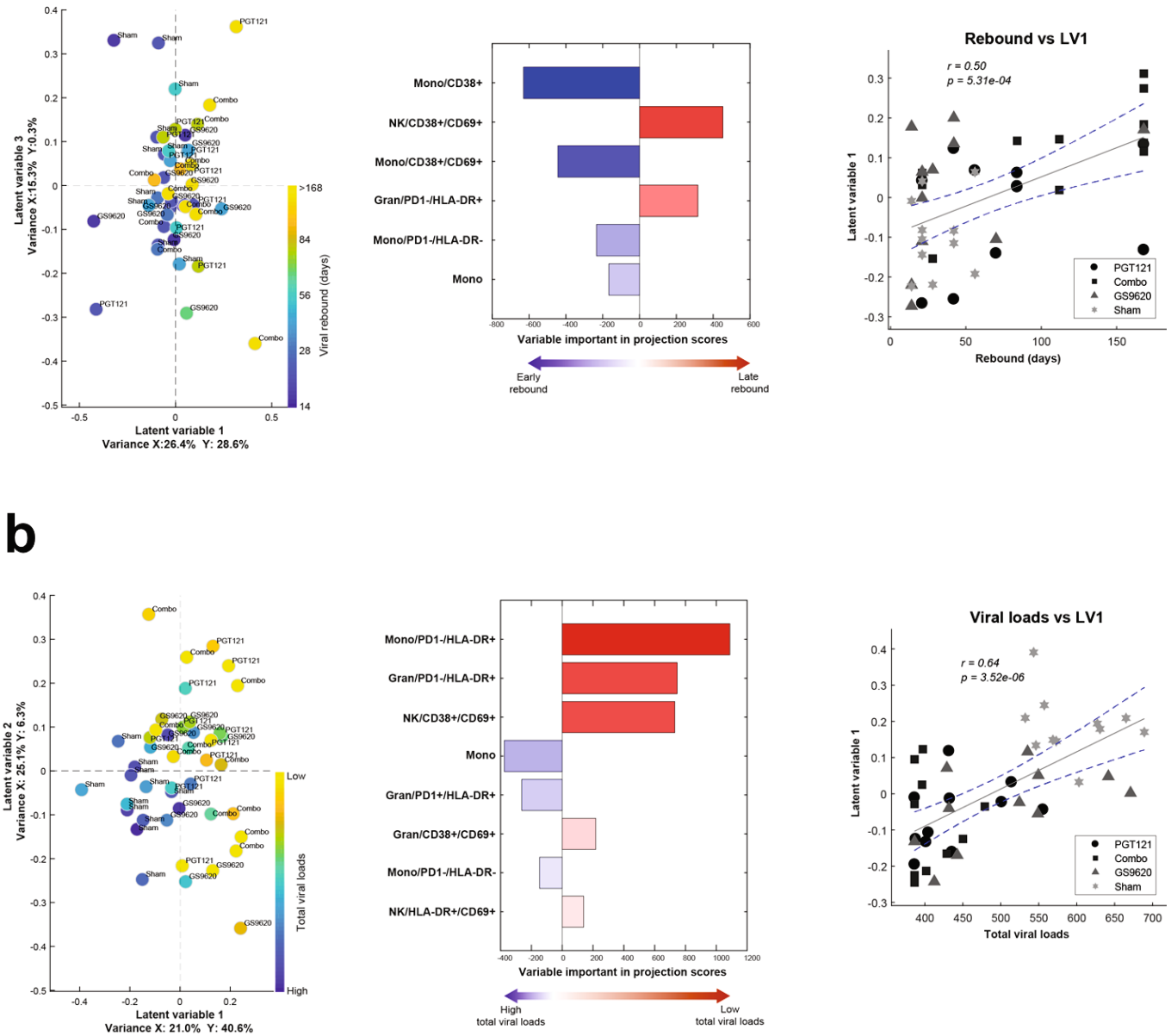

Extended Data Fig. 9 | Computational model. a, LASSO and PLSR model identifies the parameters that correlate with delayed viral rebound ($n = 11$ monkeys per group). Left, individual monkeys are shown distributed by latent variables 1 and 3 of the model. Timing of viral rebound is indicated by the colour gradient. $R^2 = 0.176$, root mean square error (RMSE) = 0.917, $P < 0.001$ in two-sided permutation tests. Middle, the contribution of the selected features to model separation is displayed in variable importance in projection (VIP) scores, related to early (blue) or late (red) viral rebound. Right, correlation between viral rebound and latent variable 1. *P* value reflects a two-sided Spearman rank-correlation test. **b**, LASSO and PLSR model identifies the parameters that correlate with reduced total viral loads ($n = 11$ monkeys per group). Left, individual monkeys are showed distributed by latent variables 1 and 2. Total viral loads are indicated by the colour gradient. $R^2 = 0.282$, root mean square error (RMSE) = 0.857, $P < 0.001$ in in two-sided permutation tests. Middle, the contribution of the selected features to model separation is displayed in VIP scores, related to high (blue) or low (red) total viral loads. Right, correlation between total viral loads and latent variable 1. *P* value reflects a two-sided Spearman rank-correlation test.

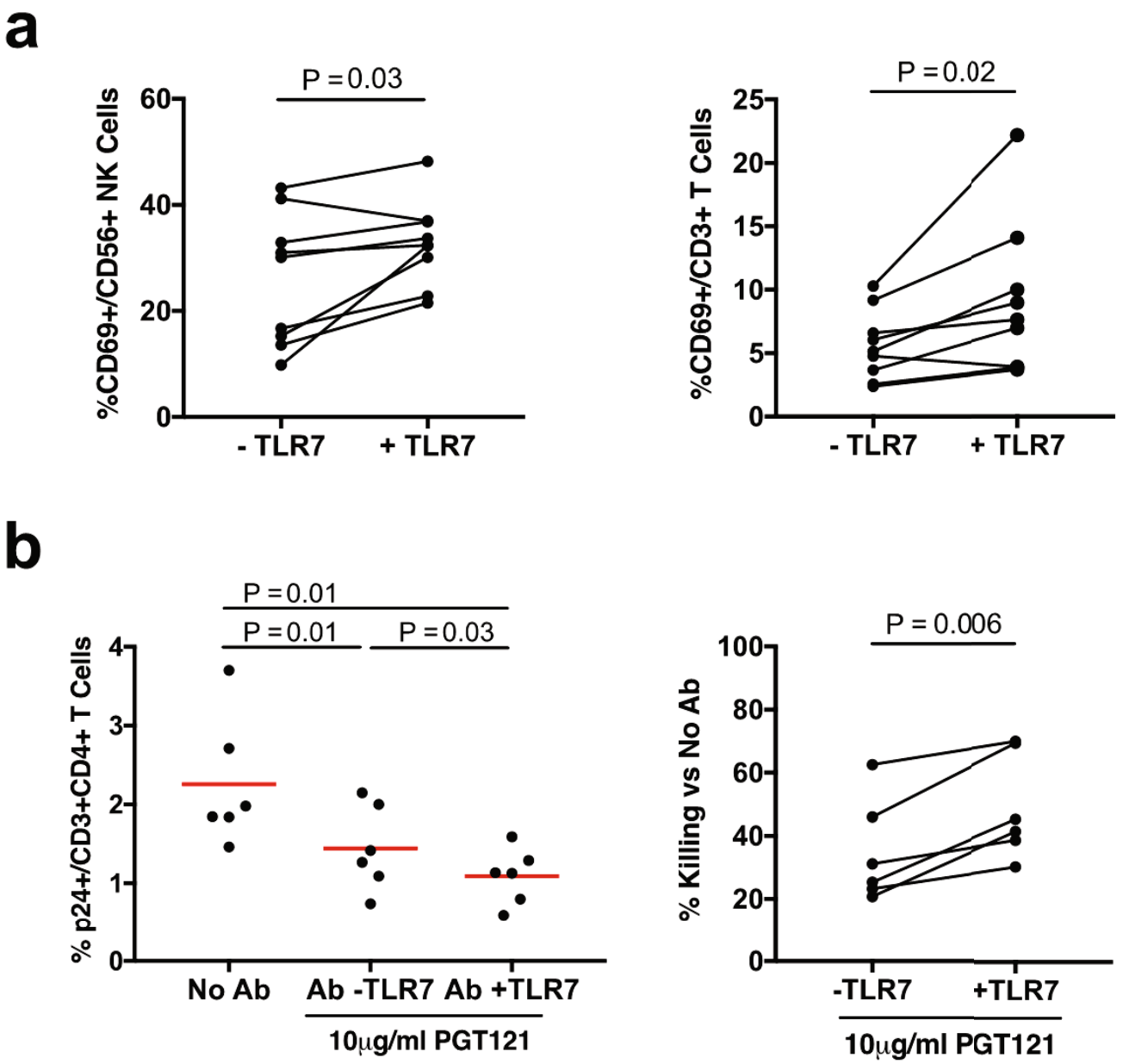

Extended Data Fig. 10 | In vitro killing studies. a, GS-9620 treatment led to CD69 upregulation of $CD56^+$ NK cells and $CD3^+$ T cells in vitro following incubation of human PBMCs with 1,000 nM GS-9620 for 5 days ($n = 9$). **b**, GS-9620 treatment augmented PGT121-mediated killing of PGT121 in vitro. Per cent p24 reduction in $CD4^+$ T cells ($n = 6$) using an antibody-mediated killing assay (see Methods). Per cent killing was calculated as the per cent reduction in p24 in $CD4^+$ T cells with PGT121 compared with no PGT121. *P* values reflect two-sided paired Student's *t*-tests.

nature research

Corresponding author(s): Dan H. Barouch

Reporting Summary

Nature Research wishes to improve the reproducibility of the work that we publish. This form provides structure for consistency and transparency in reporting. For further information on Nature Research policies, see Authors & Referees and the Editorial Policy Checklist.

Statistical parameters

When statistical analyses are reported, confirm that the following items are present in the relevant location (e.g. figure legend, table legend, main text, or Methods section).

n/a	Confirmed	
☐	☒	The exact sample size (*n*) for each experimental group/condition, given as a discrete number and unit of measurement
☐	☒	An indication of whether measurements were taken from distinct samples or whether the same sample was measured repeatedly
☐	☒	The statistical test(s) used AND whether they are one- or two-sided *Only common tests should be described solely by name; describe more complex techniques in the Methods section.*
☐	☒	A description of all covariates tested
☐	☒	A description of any assumptions or corrections, such as tests of normality and adjustment for multiple comparisons
☐	☒	A full description of the statistics including central tendency (e.g. means) or other basic estimates (e.g. regression coefficient) AND variation (e.g. standard deviation) or associated estimates of uncertainty (e.g. confidence intervals)
☐	☒	For null hypothesis testing, the test statistic (e.g. *F*, *t*, *r*) with confidence intervals, effect sizes, degrees of freedom and *P* value noted *Give P values as exact values whenever suitable.*
☒	☐	For Bayesian analysis, information on the choice of priors and Markov chain Monte Carlo settings
☒	☐	For hierarchical and complex designs, identification of the appropriate level for tests and full reporting of outcomes
☒	☐	Estimates of effect sizes (e.g. Cohen's *d*, Pearson's *r*), indicating how they were calculated
☐	☒	Clearly defined error bars *State explicitly what error bars represent (e.g. SD, SE, CI)*

Our web collection on statistics for biologists may be useful.

Software and code

Policy information about availability of computer code

Data collection	Softmax Pro version v6.5.1
Data analysis	GraphPad Prism v6.03, Cytoscape

For manuscripts utilizing custom algorithms or software that are central to the research but not yet described in published literature, software must be made available to editors/reviewers upon request. We strongly encourage code deposition in a community repository (e.g. GitHub). See the Nature Research guidelines for submitting code & software for further information.

Data

Policy information about availability of data

All manuscripts must include a data availability statement. This statement should provide the following information, where applicable:

- Accession codes, unique identifiers, or web links for publicly available datasets
- A list of figures that have associated raw data
- A description of any restrictions on data availability

Raw data on individual monkeys shown in the Figures. All data generated and analyzed in this study are available from the corresponding author upon reasonable request.

Field-specific reporting

Please select the best fit for your research. If you are not sure, read the appropriate sections before making your selection.

☒ Life sciences ☐ Behavioural & social sciences ☐ Ecological, evolutionary & environmental sciences

For a reference copy of the document with all sections, see nature.com/authors/policies/ReportingSummary-flat.pdf

Life sciences study design

All studies must disclose on these points even when the disclosure is negative.

Sample size	No formal sample size calculation was performed. A sample size of N=44 (N=11/group) was selected based on our experience to date to achive power to detect a 2-fold increase in time to viral rebound.
Data exclusions	No data were excluded.
Replication	All attempts at replication of virologic and immunologic assays were successful. Multiple timepoints were assessed to ensure reproducibility.
Randomization	Animals expressing protective MHC class I alleles and susceptible and resistant TRIM5 alleles were distributed among the groups. Animals were otherwise randomly allocated to groups.
Blinding	Immunologic and virologic assays were performed blinded.

Reporting for specific materials, systems and methods

Materials & experimental systems

n/a	Involved in the study
☐	☒ Unique biological materials
☐	☒ Antibodies
☒	☐ Eukaryotic cell lines
☒	☐ Palaeontology
☐	☒ Animals and other organisms
☒	☐ Human research participants

Methods

n/a	Involved in the study
☒	☐ ChIP-seq
☒	☐ Flow cytometry
☒	☐ MRI-based neuroimaging

Unique biological materials

Policy information about availability of materials

Obtaining unique materials	SHIV-SF162P3 and PGT121 are available by MTA from BIDMC. The ART cocktail and GS9722 are available by MTA from Gilead at their discretion.

Antibodies

Antibodies used	Catalent: PGT121 (project 3618) Becton-Dickinson: CD49d (clone 9F10), CD3 (clone SP34.2; Alexa 700), CD4 (clone L200; BV786), CD8 (clone SK1; APC H7), CD28 (clone L293, PerCP-Cy5.5), CD95 (clone DX2, BV711), CD20 (clone 2H10, BV570), CCR5 (clone 3A9, PE), BCL6 (clone K112-91, PE-CF594), CXCR5 (clone MU5UBEE, PE-cy7), and PD-1 (clone EH12.2H7, Pacific Blue), IFN-g (clone B27; BUV395), IL-2 (clone MQ1-17H12; BUV737), TNF-a (clone Mab11; BV650), CD69 (clone FN50, BV510), Ki67 (clone B56, FITC)
Validation	All antibodies were used per manufacturer's instructions and confirmed for reactivity for rhesus monkey samples.

Animals and other organisms

Policy information about studies involving animals; ARRIVE guidelines recommended for reporting animal research

Laboratory animals	M. mulatta, mixed male and female, age 3-8 years

Wild animals	The study did not involve wild animals.
Field-collected samples	The study did not involve samples collected from the field.